Supplementary Information

Control of structure topology and spatial distribution of biomacromolecules in protein@ZIF-8 biocomposites

Weibin Liang[†], Raffaele Ricco[‡], Natasha K. Maddigan[†], Robert P. Dickinson[†], Huoshu Xu[§], Qiaowei Li[§], Christopher J. Sumby[†], Stephen G. Bell[†], Paolo Falcaro*[‡†], Christian J. Doonan*[†]

[†]Department of Chemistry and the Centre for Advanced Nanomaterials, The University of Adelaide, Adelaide, South Australia 5005, Australia

[‡]Institute of Physical and Theoretical Chemistry, Graz University of Technology, Stremayrgasse 9, Graz 8010, Austria

[§]Department of Chemistry, iChEM (Collaborative Innovation Center of Chemistry for Energy Materials), and Shanghai Key Laboratory of Molecular Catalysis and Innovative Materials, Fudan University, Shanghai 200433, P.R. China

Table of Content

S1 Synthesis parameter screening for biomimetic mineralized growth of ZIF phases

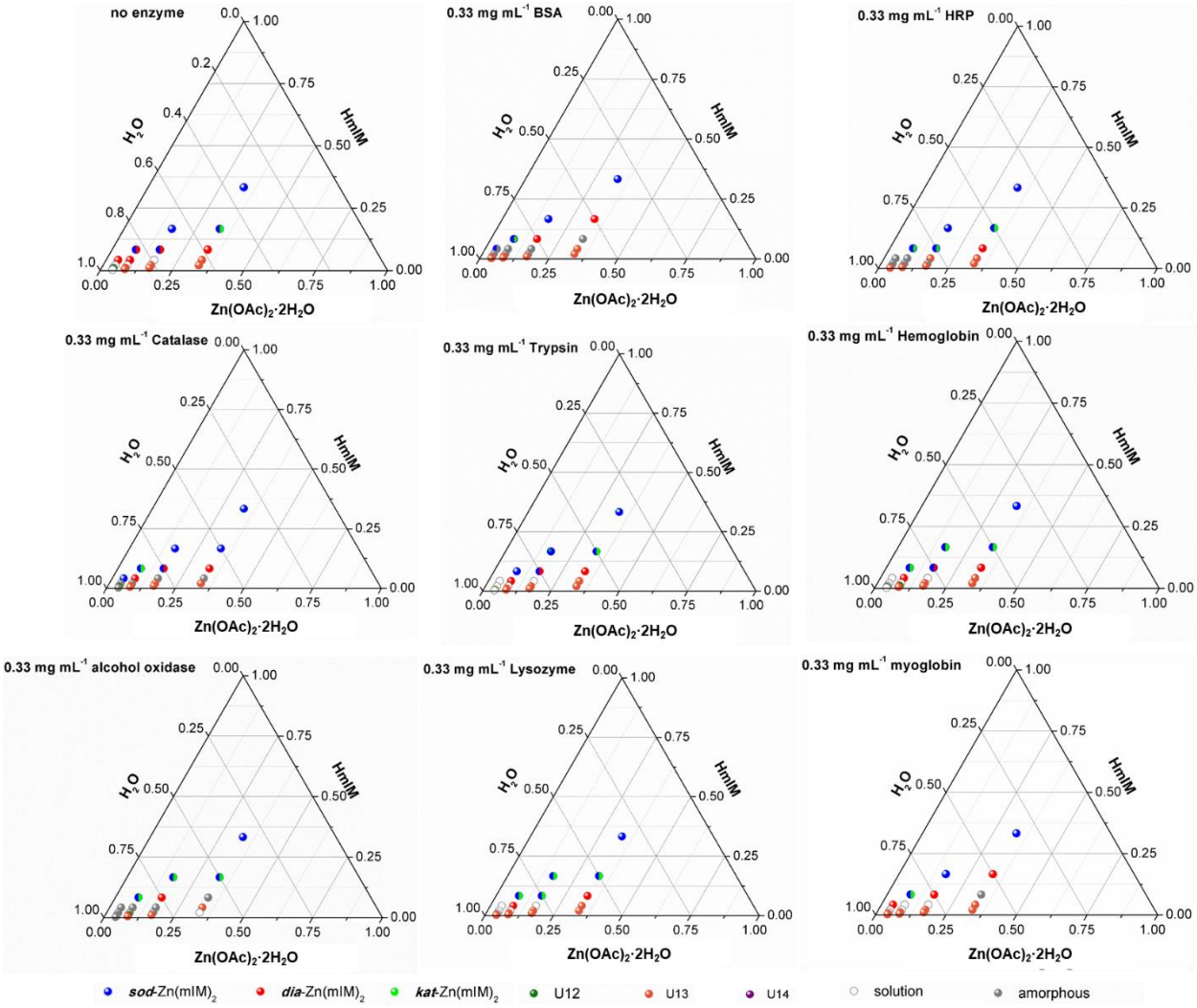

Figure S1. Ternary graphs (volumetric fraction; the volume of the reaction mixture is 3 mL, non-stirred samples) of deionized water (or 0.33 mg mL^{-1} aqueous solution of protein/enzyme (bovine serum albumin (BSA), horseradish peroxidase (HRP), catalase, trypsin, hemoglobin, alcohol oxidase, lysozyme and myoglobin), 0.24 M aqueous solution of $Zn(OAc)_2{\cdot}2H_2O$, and 3.84 M aqueous solution of 2-methylimidazole (HmIM) showing the metal-organic framework (MOF) phase diagram at different $Zn(OAc)_2{\cdot}2H_2O$ concentration (80 mM, 40 mM, 20 mM, and 10 mM) and molar ratio between Zn^{2+} and HmIM ($HmIM/Zn^{2+}$ = 16, 8, 4, 2, and 1). The reaction mixture was kept at room temperature without stirring for 24 h. After synthesis, the precipitates were collected by centrifugation (10,000 rpm for 5 min), air-dried, and measured by PXRD without washing.

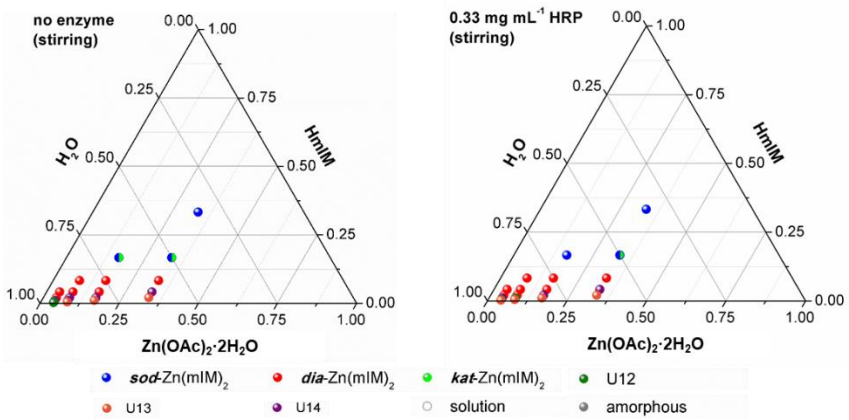

Figure S2. Ternary graphs (volumetric fraction; the volume of the reaction mixture is 3 mL, stirred samples) of deionized water (or 0.33 mg mL^{-1} aqueous solution of horseradish peroxidase (HRP)), 0.24 M aqueous solution of $Zn(OAc)_2{\cdot}2H_2O$, and 3.84 M aqueous solution of 2-methylimidazole (HmIM) showing the metal-organic framework (MOF) phase diagram at different $Zn(OAc)_2{\cdot}2H_2O$ concentration (80 mM, 40 mM, 20 mM, and 10 mM) and molar ratio between Zn^{2+} and HmIM ($HmIM/Zn^{2+}$ = 16, 8, 4, 2, and 1). The reaction mixture was stirred at room temperature for 24 h. After synthesis, the precipitates were collected by centrifugation (10,000 rpm for 5 min), air-dried, and measured by PXRD without washing.

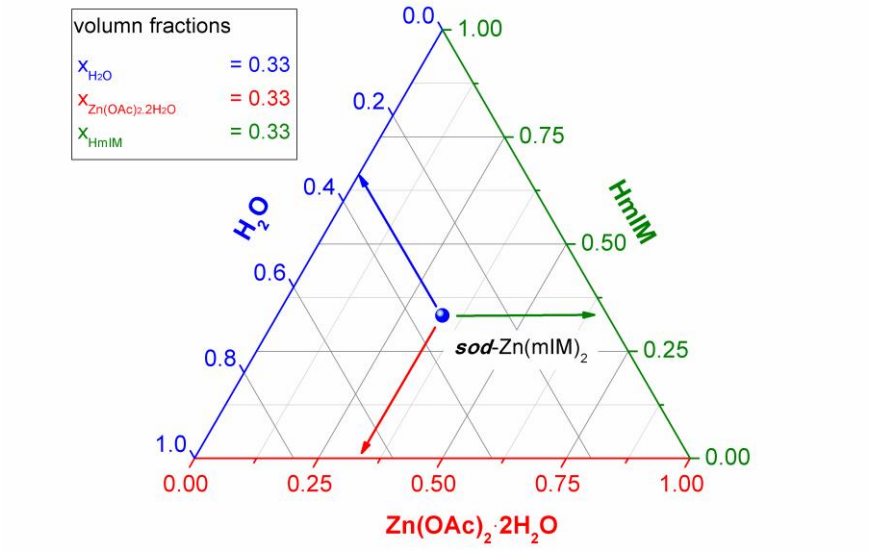

Figure S3. A generic example to demonstrate the interpretation of ternary graphs (by volumetric fraction of deionized water (or 0.33 mg mL^{-1} aqueous solution of biomacromolecule), 0.24 M aqueous solution of $Zn(OAc)_2{\cdot}2H_2O$, and 3.84 M aqueous solution of 2-methylimidazole (HmIM); the total volume of the reaction mixture is 3 mL). In the example shown, the volumes of H_2O, 0.24 M aqueous solution of $Zn(OAc)_2{\cdot}2H_2O$, and 3.84 M aqueous solution of HmIM used in the reaction mixture are 1, 1, and 1 mL ($V_{H2O} = X_{H2O}$ x 3 mL, $V_{Zn(OAc)2{\cdot}2H2O} = X_{Zn(OAc)2{\cdot}2H2O}$ x 3 mL, $V_{HmIM} = X_{HmIM}$ x 3 mL), respectively.

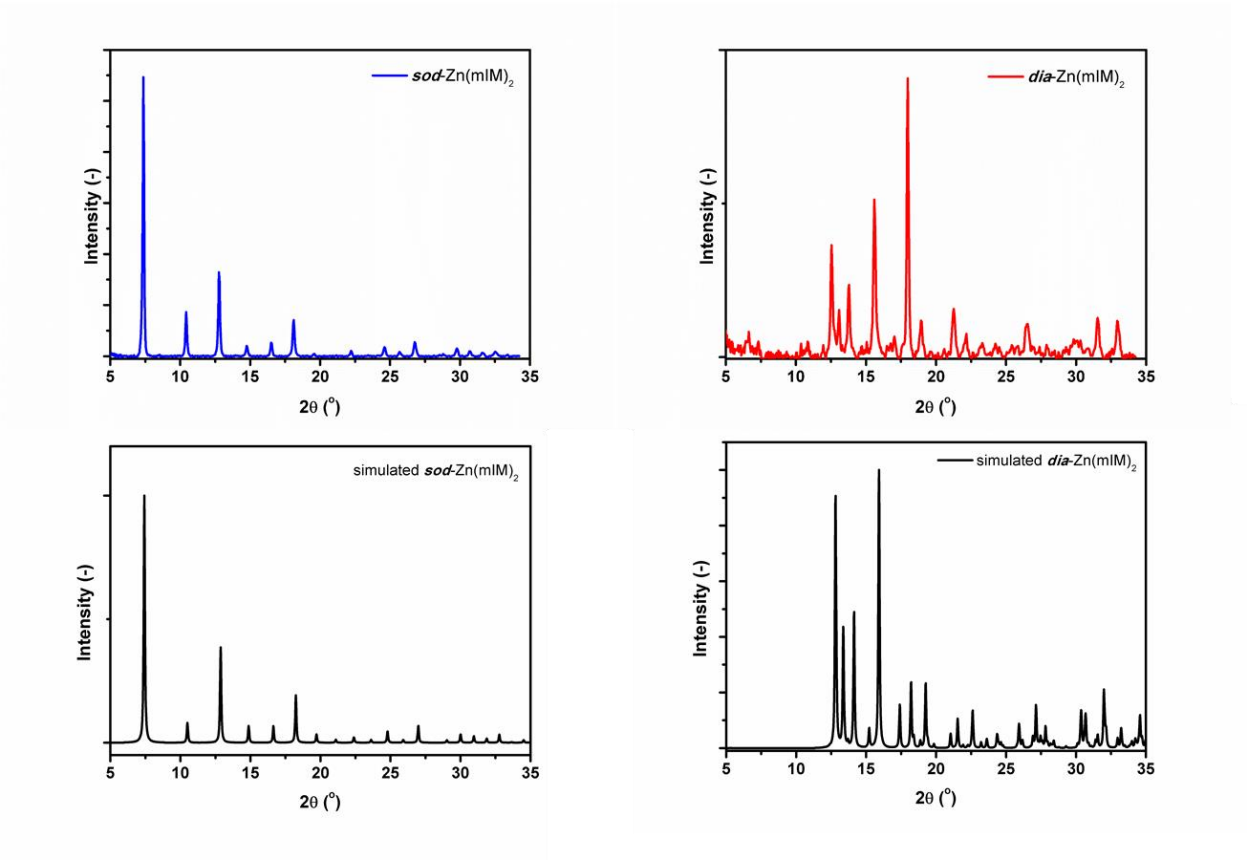

Figure S4. Experimental and simulated PXRD patterns for ***sod***-Zn(mIM)$_2$ and ***dia***-Zn(mIM)$_2$.

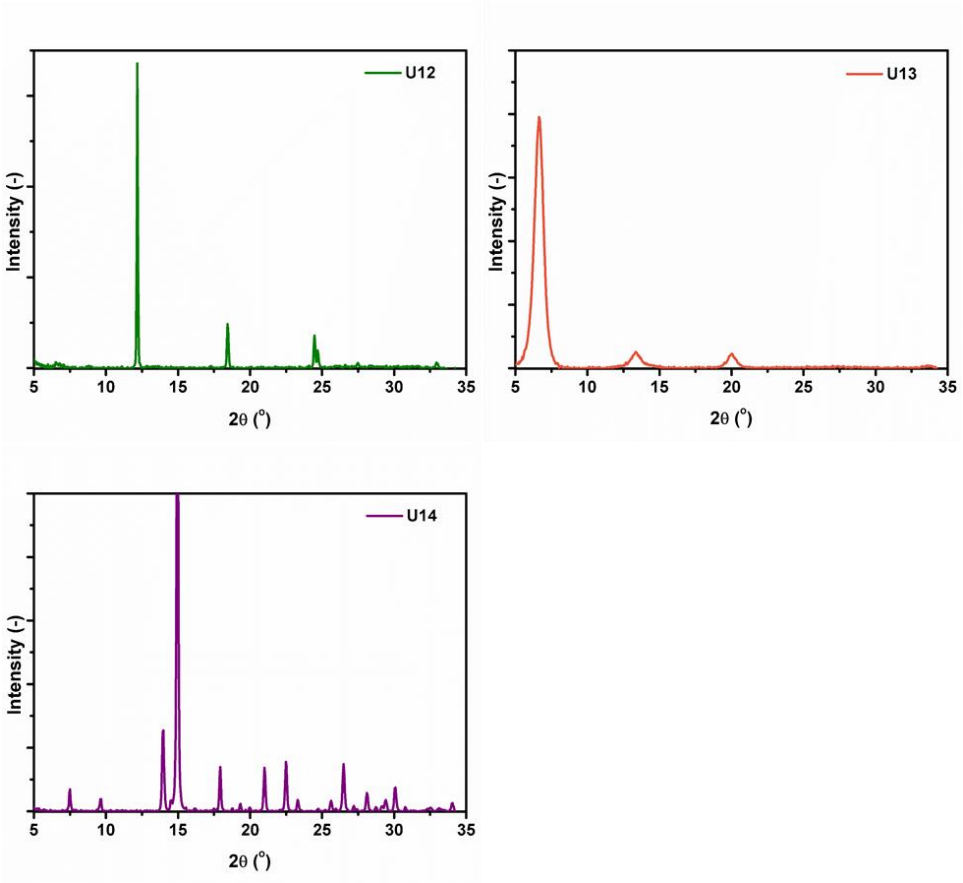

Figure S5. Experimental PXRD patterns for U12, U13, and U14.

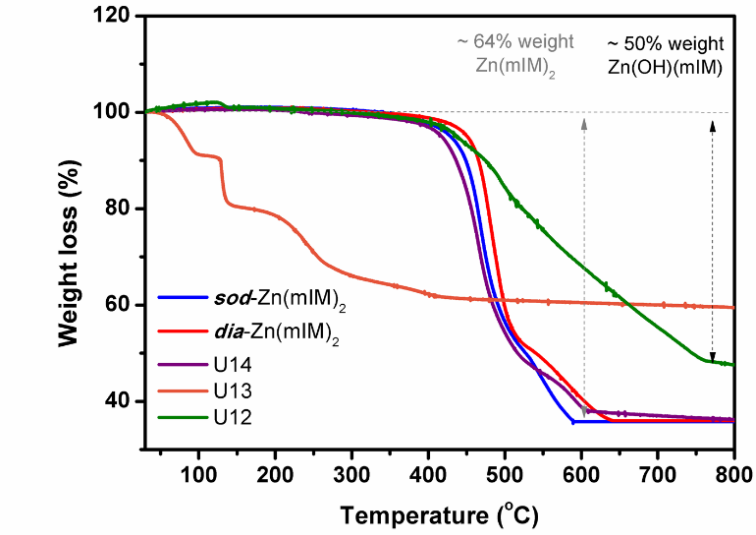

Figure S6. Thermogravimetric analysis (TGA) showing the weight loss for ***sod***-$Zn(mIM)_2$, ***dia***-$Zn(mIM)_2$, U12, U13, and U14.

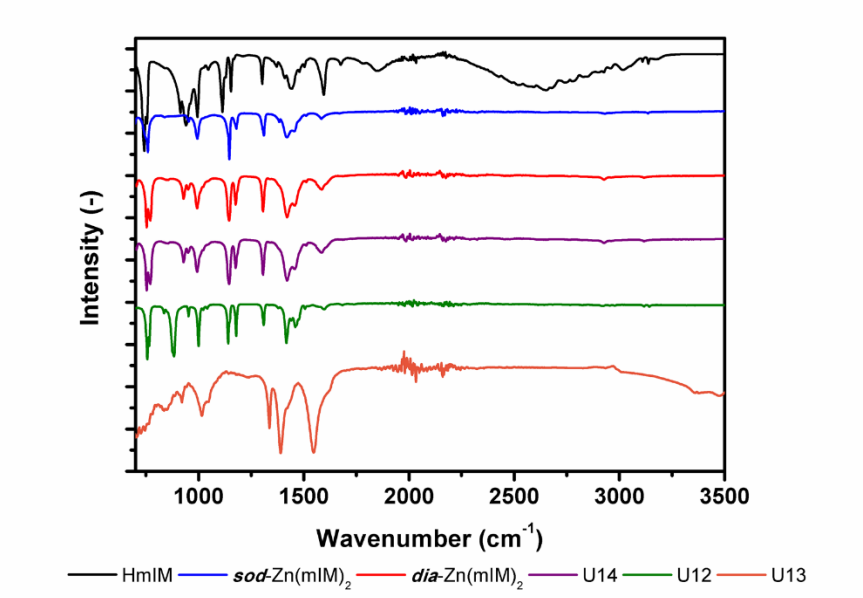

Figure S7. FTIR spectra for ***sod***-Zn(mIM)$_2$, ***dia***-Zn(mIM)$_2$, U12, U13, and U14.

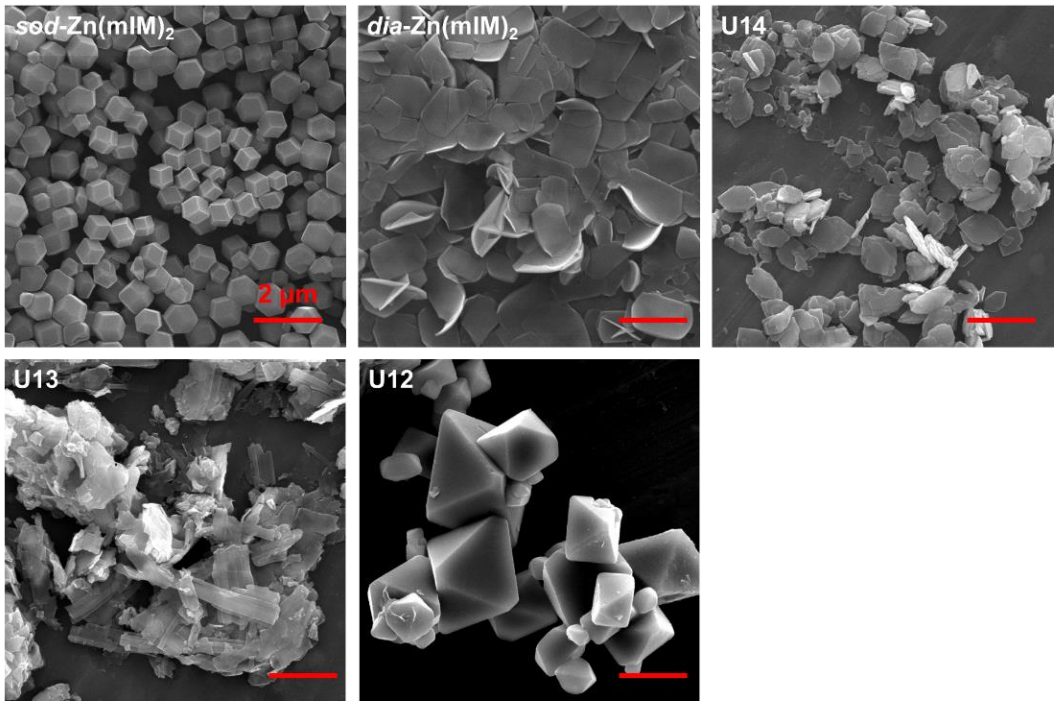

Figure S8. Scanning electron microscopy images for ***sod***-Zn(mIM)$_2$, ***dia***-Zn(mIM)$_2$, U12, U13, and U14.

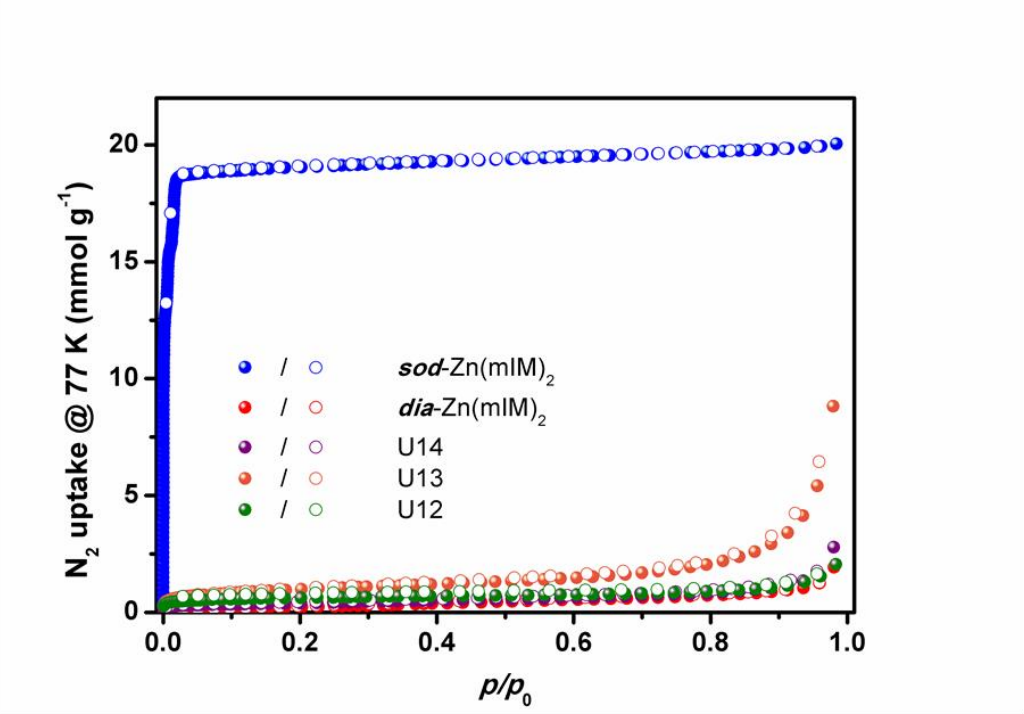

	sod-Zn(mIM)$_2$	***dia***-Zn(mIM)$_2$	U14	U13	U12
S_{BET} (m^2 g^{-1})	1358.5 ± 2.3	22.9 ± 0.5	26.0 ± 0.5	79.8 ± 0.2	50.9 ± 0.1

Figure S9. 77K N_2 adsorption (filled symbol) desorption (open symbol) isotherms for ***sod***-Zn(mIM)$_2$ (blue), ***dia***-Zn(mIM)$_2$ (red), U12 (green), U13 (orange), and U14 (purple). The calculated BET surface areas for samples are listed.

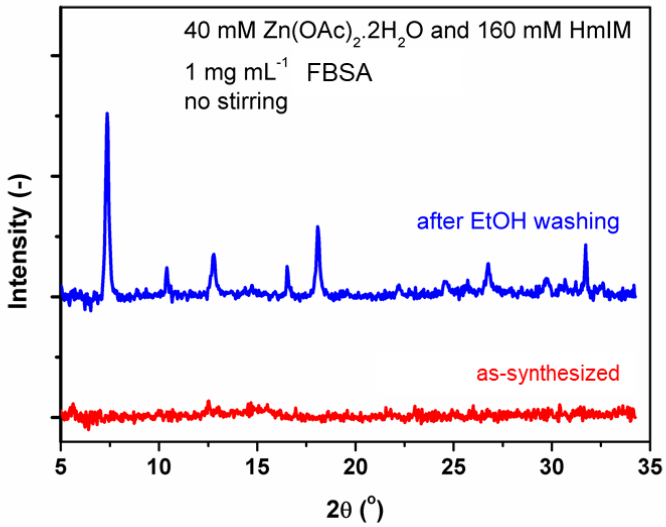

Figure S10. Experimental PXRD patterns of as-synthesized amorphous product (baseline corrected using X'Pert HighScore Plus software) and the FBSA-**@**-***sod***-Zn(mIM)$_2$ transformed from the amorphous product by ethanol washing. Synthesis conditions for the material are listed in the graph.

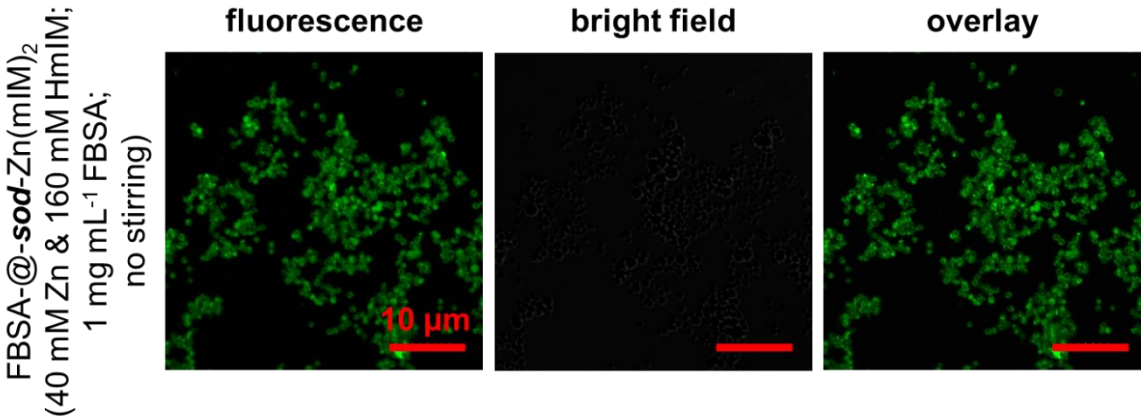

Figure S11. Confocal laser scanning micrographs showing the fluorescence, bright field, and overlay images of FBSA-**@**-***sod***-Zn(mIM)$_2$, which was synthesized in water with 40 mM of $Zn(OAc)_2{\cdot}2H_2O$, 160 mM of HmIM and 1 mg mL^{-1} of FBSA at room temperature under static conditions for 24 h. The precipitate was initially amorphous, which can transform into crystalline ***sod***-Zn(mIM)$_2$ by ethanol washing.

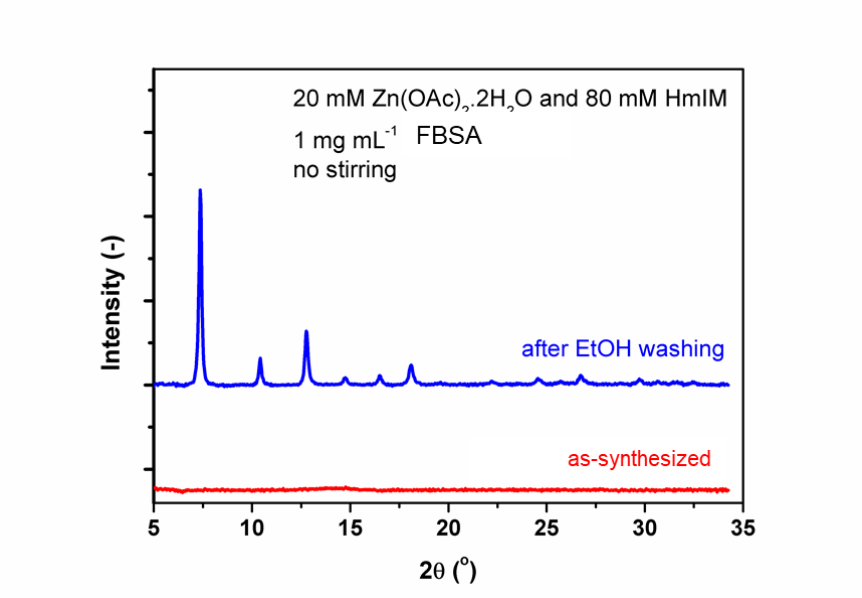

Figure S12. Experimental PXRD patterns of as-synthesized amorphous product (baseline corrected using X'Pert HighScore Plus software) and the FBSA-**@**-***sod***-Zn(mIM)$_2$ transformed from the amorphous product by ethanol washing. Synthesis conditions for the material are listed in the graph.

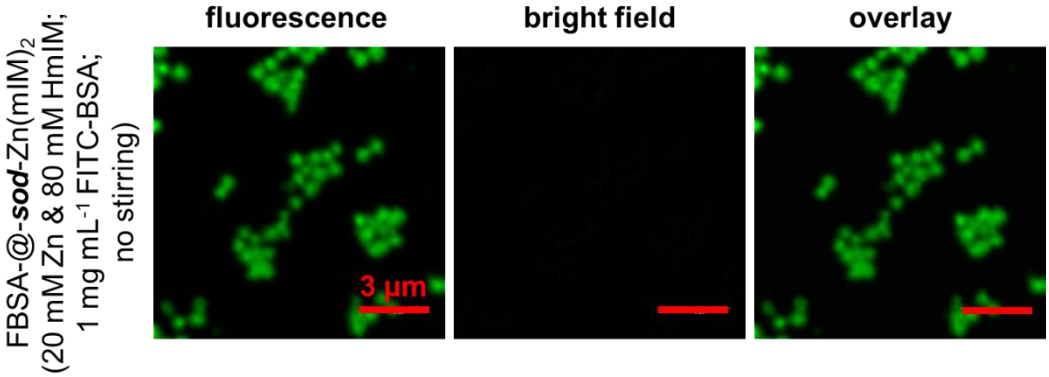

Figure S13. Confocal laser scanning micrographs showing the fluorescence, bright field, and overlay images of FBSA-**@**-***sod***-Zn(mIM)$_2$, which was synthesized in water with 20 mM of $Zn(OAc)_2 \cdot 2H_2O$, 80 mM of HmIM and 1 mg mL^{-1} of FBSA at room temperature under static conditions for 24 h. The precipitate was initially amorphous, which can transform into crystalline ***sod***-Zn(mIM)$_2$ by ethanol washing.

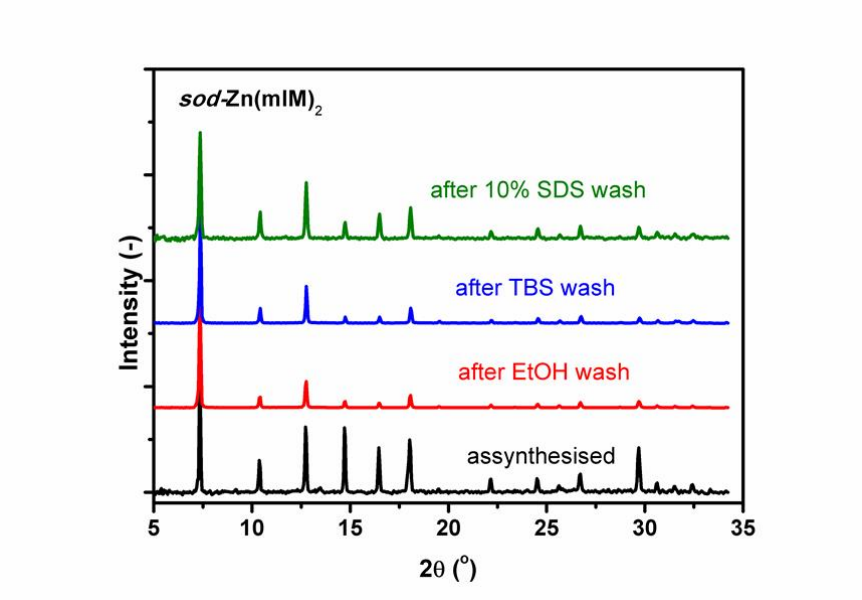

Figure S14. Experimental PXRD patterns of as-synthesized ***sod***-$Zn(mIM)_2$ (black), and ***sod***-$Zn(mIM)_2$ after ethanol (red), TBS buffer (50 mM Tris base and 150 mM NaCl in water, pH 7.5; blue), and 10% SDS (w/w in pH 7.5 TBS buffer; green) washing.

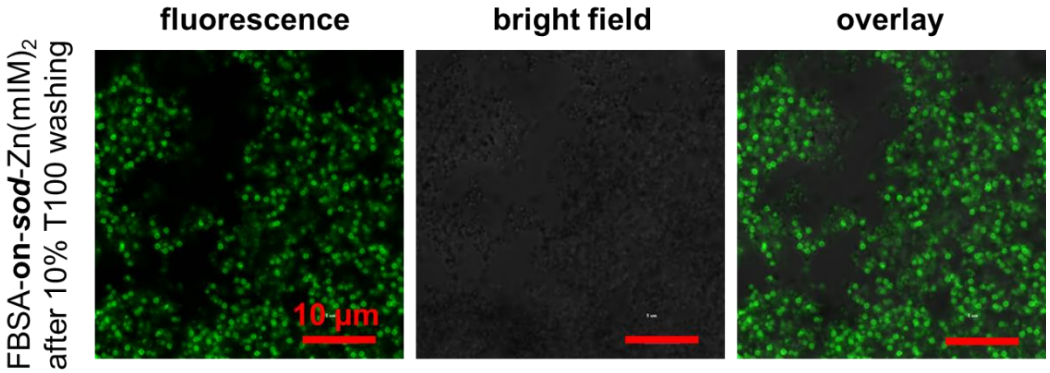

Figure S15. Confocal laser scanning micrographs showing the fluorescence, bright field, and overlay images of FBSA-**on**-***sod***-$Zn(mIM)_2$ after 10% T100 washing (w/w; T100 = Triton™ X100; in pH 7.5 TBS buffer).

S2. Effect of synthesis parameters on FBSA/sod-Zn(mIM)$_2$ biocomposites

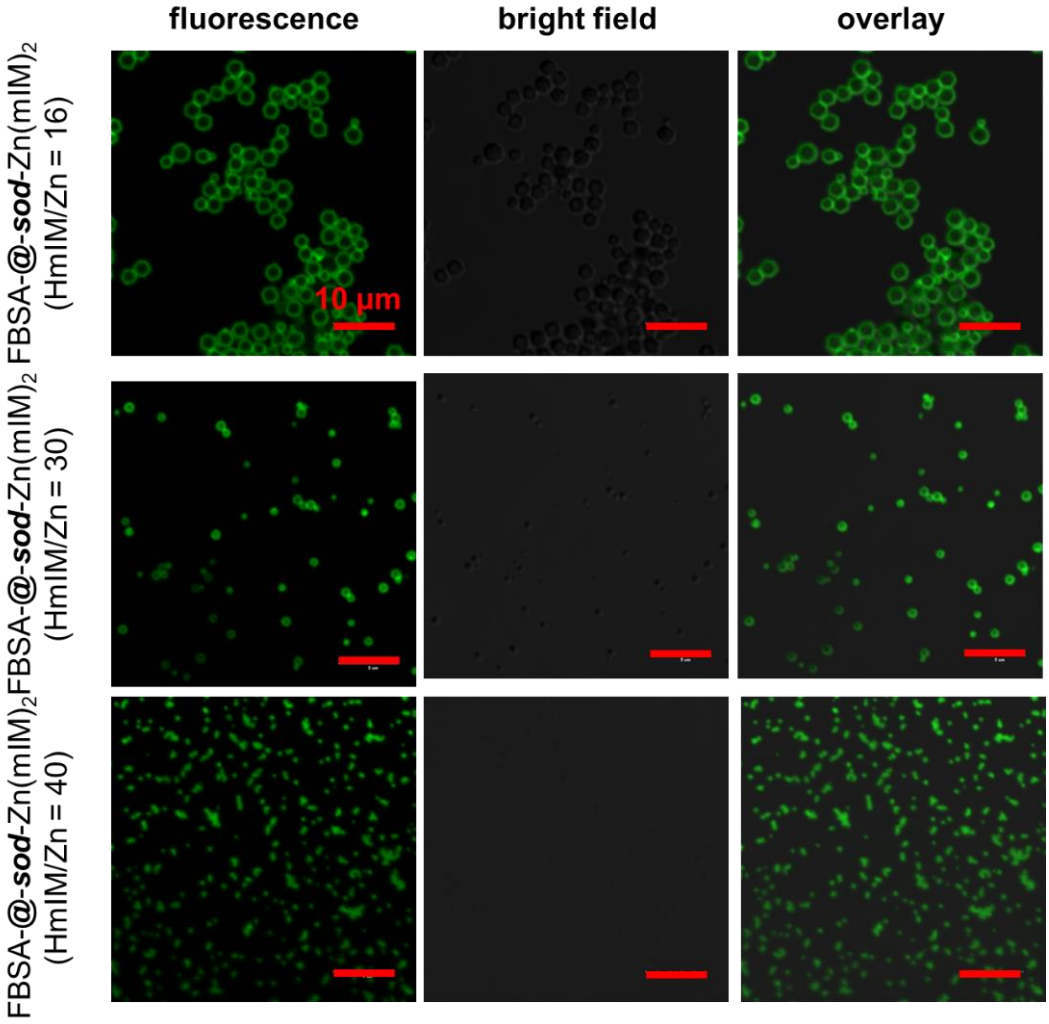

Figure S16. Confocal laser scanning micrographs showing the fluorescence, bright field, and overlay images of FBSA-***@-sod***-Zn(mIM)$_2$, which was synthesized in water with 40 mM of $Zn(OAc)_2{\cdot}2H_2O$, 640 mM of HmIM (1200 mM for HmIM/Zn = 30 sample and 1600 mM for HmIM/Zn = 40 sample) and 0.33 mg mL^{-1} FBSA at room temperature under static conditions for 24 h. The precipitate was recovered by centrifugation at 10,000 rpm for 5 min and then washed, sonicated, and centrifuged twice each in pH 7.5 TBS buffer followed by ethanol. Thereafter, sample was washed with 10% SDS solution (2x; w/w; in pH 7.5 TBS buffer) to remove surface adsorbed FITC-BSA followed by pH 7.5 TBS buffer (2x) and ethanol (2x) to remove residue surfactant. Scale bar for all images are 10 µm.

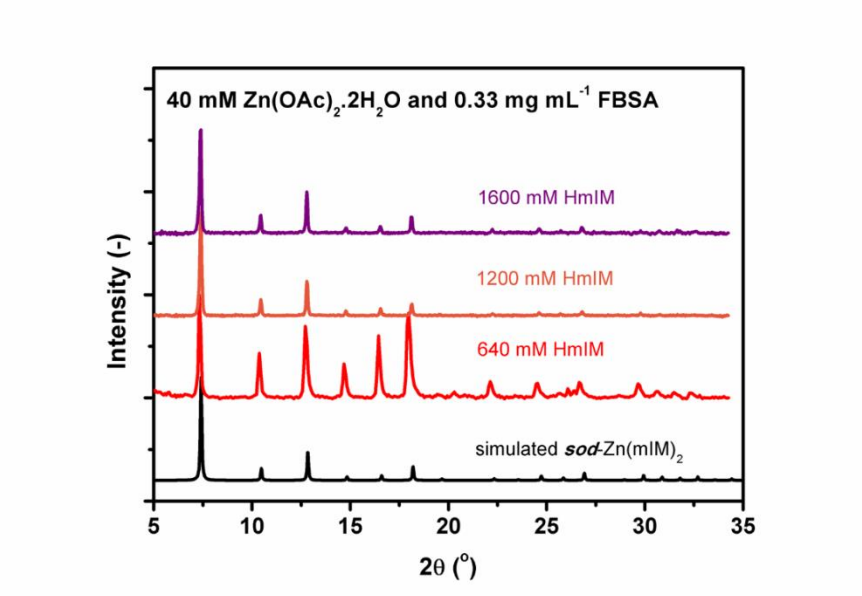

Figure S17. Simulated PXRD pattern for ***sod***-$Zn(mIM)_2$ and experimental PXRD patterns for FBSA-***@-sod***-$Zn(mIM)_2$ synthesized using 40 mM of $Zn(OAc)_2{\cdot}2H_2O$, 0.33 mg mL^{-1} FBSA and different concentration of HmIM (640, 1200, and 1600 mM) under static conditions.

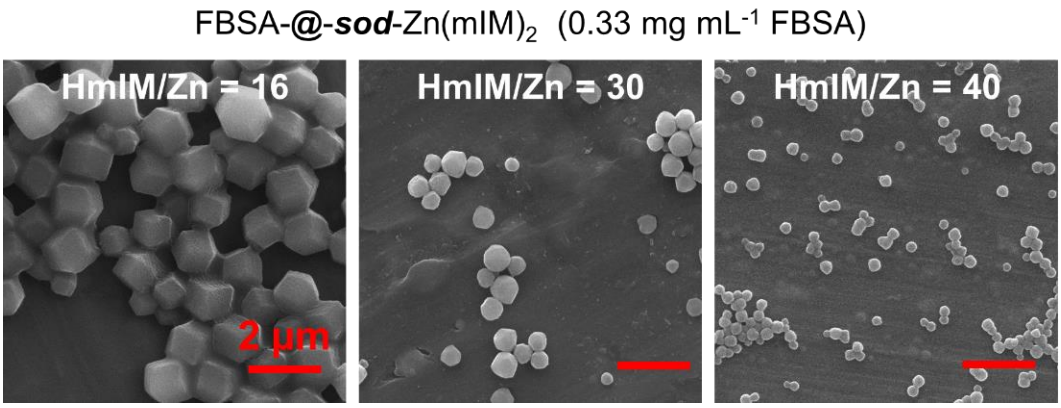

Figure S18. SEM images for FBSA-***@-sod***-$Zn(mIM)_2$ synthesized using 40 mM of $Zn(OAc)_2{\cdot}2H_2O$, 0.33 mg mL^{-1} FBSA and different concentration of HmIM (640, 1200, and 1600 mM) under static conditions. Particle size for samples synthesized using HmIM/Zn ratio of 16, 30, and 40 were calculated to be 1.58 ± 0.15, 0.69 ± 0.12, and 0.38 ± 0.04 µm, respectively.

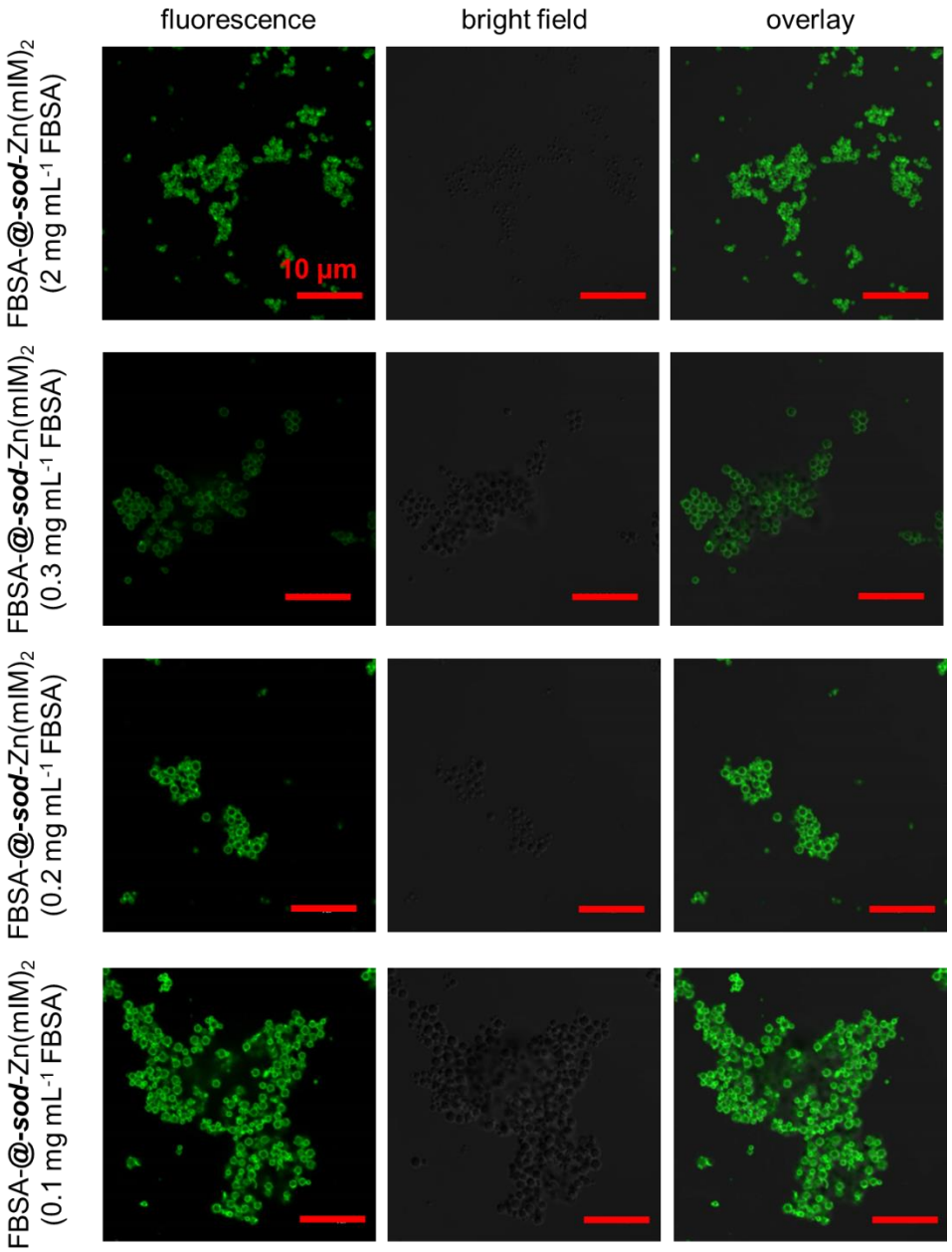

Figure S19. Confocal laser scanning micrographs showing the fluorescence, bright field, and overlay images of FBSA-**@-*sod***-Zn(mIM)$_2$, which was synthesized in water with 40 mM of Zn(OAc)$_2$·2H$_2$O, 640 mM of HmIM and different concentration of FBSA (0.1, 0.2, 0.33, and 2 mg mL^{-1}) at room temperature under stirring for 24 h. The precipitate was recovered by centrifugation at 10,000 rpm for 5 min and then washed, sonicated, and centrifuged twice each in pH 7.5 TBS buffer followed by ethanol. Thereafter, sample was washed with 10% SDS solution (2x; w/w; in pH 7.5 TBS buffer) to remove surface adsorbed FITC-BSA followed by pH 7.5 TBS buffer (2x) and ethanol (2x) to remove residue surfactant. Scale bar for all images are 10 µm.

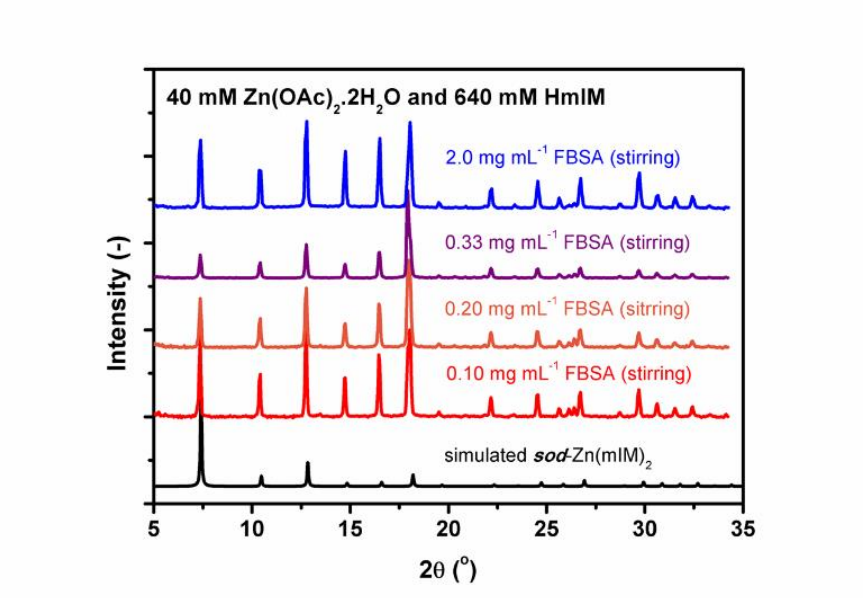

Figure S20. Simulated PXRD pattern for ***sod***-$Zn(mIM)_2$ and experimental PXRD patterns for FBSA-***@-sod***-$Zn(mIM)_2$ synthesized using 40 mM of $Zn(OAc)_2{\cdot}2H_2O$, 640 mM of HmIM and different concentration of FBSA (0.10, 0.20, 0.33, and 2.0 mg mL^{-1} FBSA) under stirred conditions.

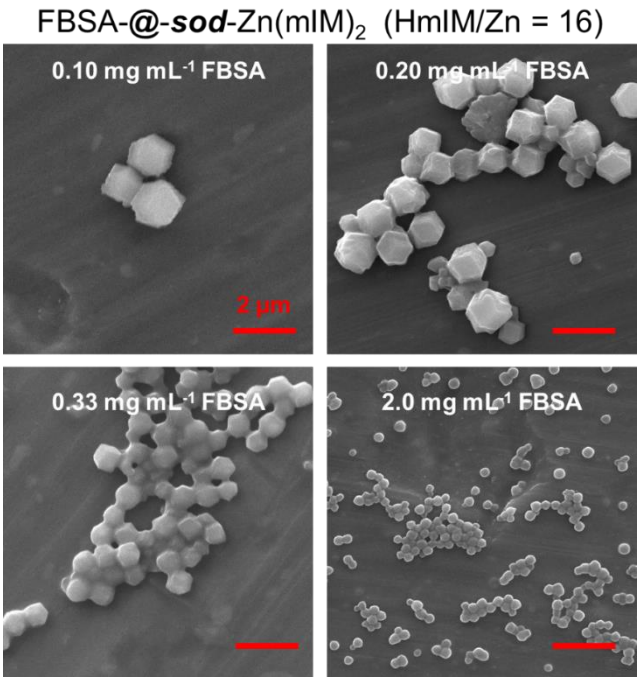

Figure S21. SEM images for FBSA-***@-sod***-$Zn(mIM)_2$ synthesized using 40 mM of $Zn(OAc)_2{\cdot}2H2O$, 640 mM of HmIM and different concentration of FBSA (0.10, 0.20, 0.33, and 2.0 mg mL^{-1} FBSA) under stirred conditions. Particle size for samples synthesized using 0.10, 0.20, 0.33, and 2.0 mg mL^{-1} FBSA were calculated to be 1.53 ± 0.23, 1.47 ± 0.14, 1.33 ± 0.14, and 0.84 ± 0.06 μm, respectively.

S3. Effect of protein-modification on the biomolecules spatial distribution within the *sod*-Zn(mIM)$_2$

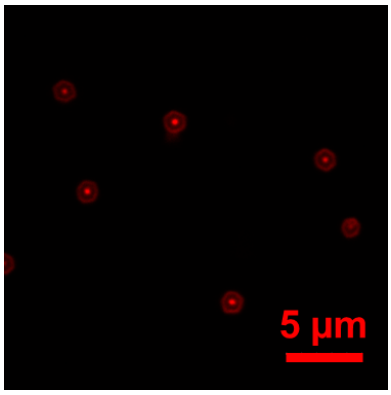

Figure S22. CLSM fluorescence images of RbBSA-***@-sod***-Zn(mIM)$_2$, which was synthesized in water with 40 mM of $Zn(OAc)_2 \cdot 2H_2O$, 640 mM of HmIM and 0.33 mg mL^{-1} of FBSA at room temperature under static conditions for 24 h.

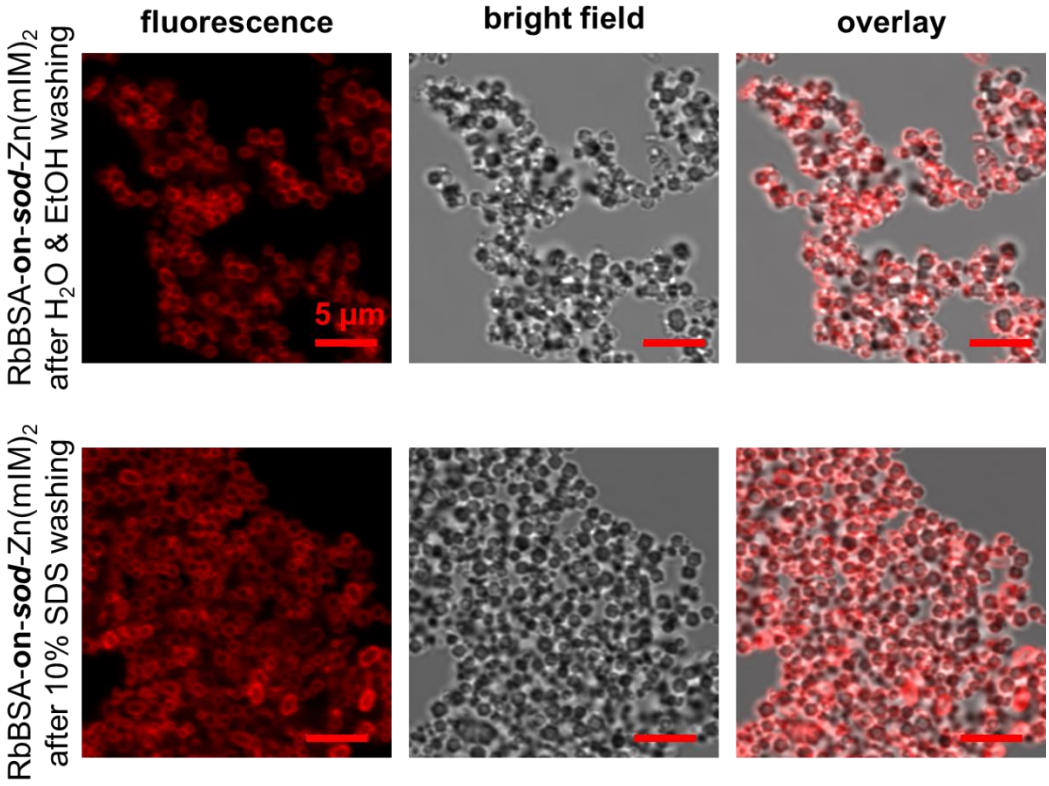

Figure S23. Confocal laser scanning micrographs showing the fluorescence, bright field, and overlay images of RbBSA-**on**-***sod***-Zn(mIM)$_2$ after H_2O and EtOH washing and FBSA-**on**-***sod***-Zn(mIM)$_2$ after 10% SDS washing (60 °C for 24 h).

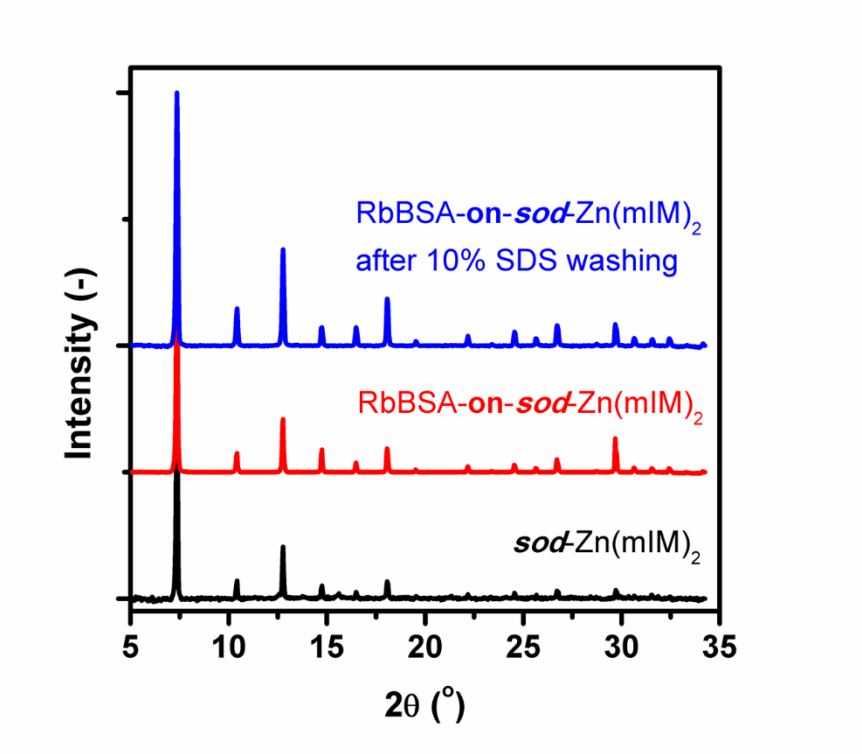

Figure S24. Experimental PXRD patterns of as-synthesized ***sod***-$Zn(mIM)_2$ (black), as-synthesized RbBSA-**on**-***sod***-$Zn(mIM)_2$ (red), and RbBSA-**on**-***sod***-$Zn(mIM)_2$ after 10% SDS treatment.

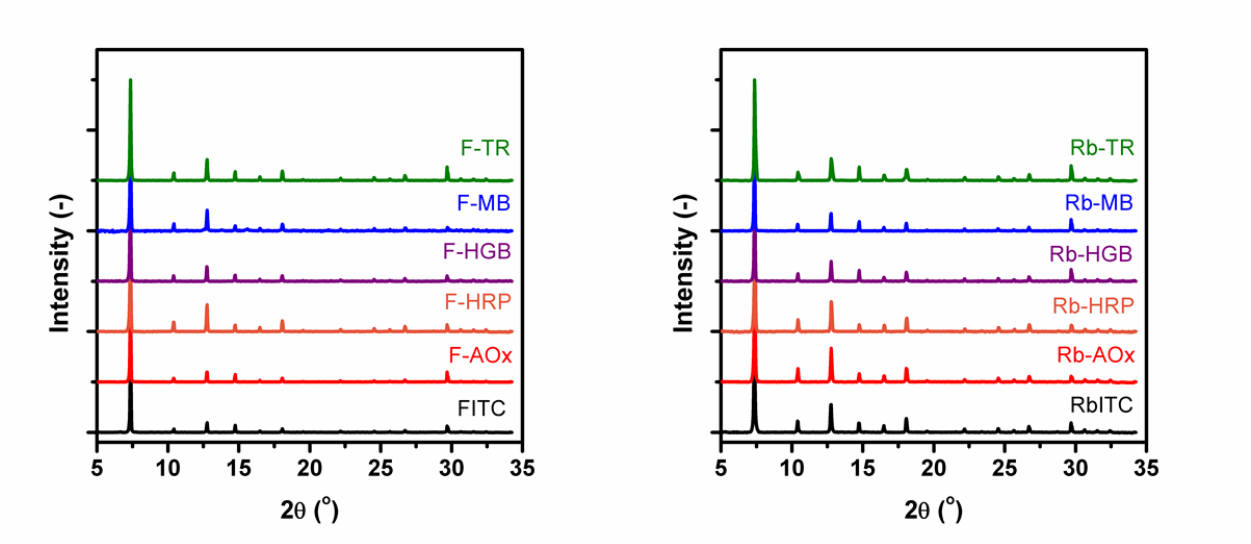

Figure S25. Experimental PXRD patterns of ***sod***-$Zn(mIM)_2$ synthesized in the presence of FITC, rhodamine B, and fluorescein- (or rhodamine B-) tagged AOx (F-AOx, or Rb-AOx), HRP (F-HRP or Rb-HRP), HGB (F-HGB or Rb-HGB), MB (F-MB or Rb-MB), trypsin (F-TR or Rb-TR).

S4. Quantification of FBSA within FBSA/sod-Zn(mIM)$_2$ composites

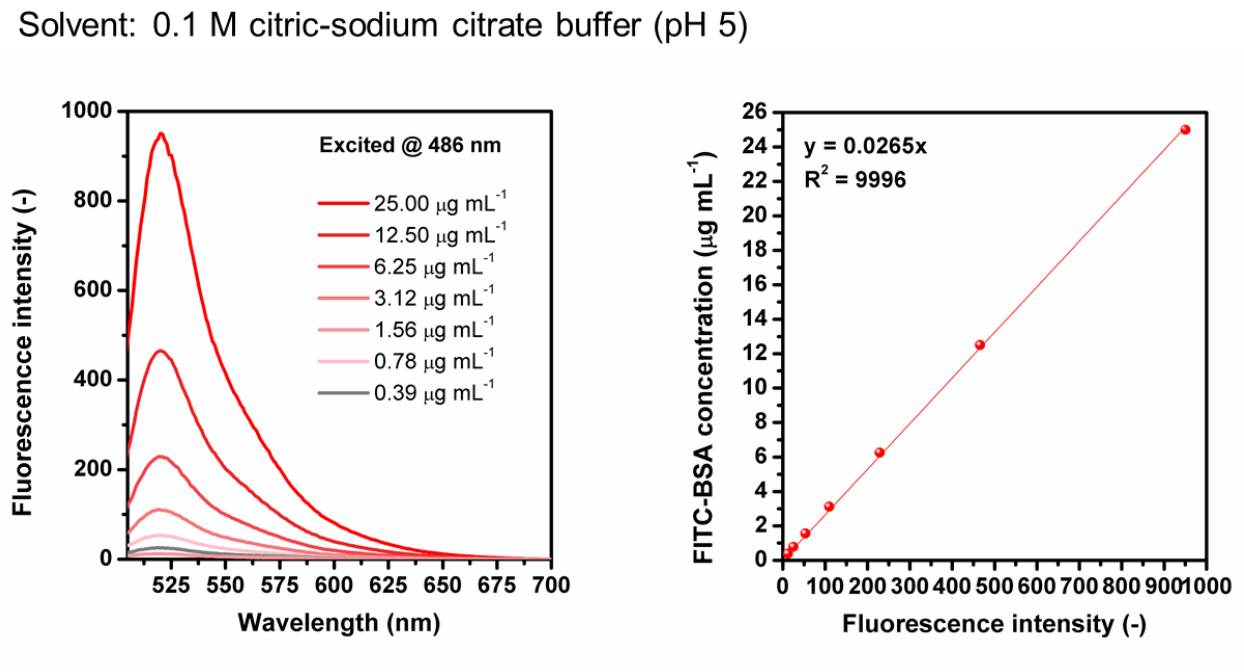

Figure S26. Calibration curve for FBSA in 0.1 M citric-sodium citrate buffer (pH 5).

Table S1 FBSA loading and immobilization efficiency of FBSA in FBSA-***@-sod***-Zn(mIM)$_2$ samples (synthesized with different amount of FBSA) before and after 10% SDS treatment.

Entry[a]	FBSA dosage in synthesis solution [mg][d]	Calculated FBSA loading [wt%][e]	Experimental FBSA loading [wt%][f]	FBSA immobilization efficiency [%][g]
FBSA-@-sod$_{0.3}$[b]	0.3	1.1	0.9(0.04)	88.9
FBSA-@-sod$_{0.6}$[b]	0.6	2.1	1.8(0.07)	84.6
FBSA-@-sod$_{1}$[b]	1.0	3.5	2.6(0.20)	74.0
FBSA-@-sod$_{0.3, SDS}$[c]	0.3	1.1	0.5(0.01)	45.4
FBSA-@-sod$_{0.6, SDS}$[c]	0.6	2.1	0.8(0.07)	38.8
FBSA-@-sod$_{1, SDS}$[c]	1.0	3.5	1.1(0.03)	32.3

[a]FBSA = fluorescein-tagged bovine serum albumin; FBSA-@-sod$_x$ = FBSA-***@-sod***-Zn(mIM)$_2$, x = FBSA amount used in the composite syntheses;
[b]After synthesis, the composites were recovered by centrifugation, washed twice with water (x2) then ethanol (x2), and dried under vacuum prior to further analysis;
[c]The ethanol washed, dried FBSA-***@-sod***-Zn(mIM)$_2$ samples were dispersed in 10% SDS solution (w/w, in pH 7.5 TBS buffer; SDS = sodium dodecyl sulfate) by sonication and left for 30 min at room temperature. Then, the samples were washed twice with water followed by twice with ethanol. Thereafter, the samples were dried under vacuum and storage at 4 °C prior to further analysis;
[d]Samples were synthesized with 40 mM of $Zn(OAc)_2{\cdot}2H_2O$, 640 mM of HmIM and different dosage of FBSA in water at room temperature under stirring for 24 h;
[e]Calculated FBSA loading (wt%) = $m_{FBSA}/(m_{FBSA} + m_{sod})$; the yield of ***sod***-Zn(mIM)$_2$ (based on Zn) was estimated from the same synthesis conditions as FBSA-***@-sod***-Zn(mIM)$_2$ without FBSA addition (~100%);
[f]FBSA-***@-sod***-Zn(mIM)$_2$ samples were dissolved in 0.1 M carbonate-bicarbonate buffer solution. The FBSA amount was quantified by fluorescence spectroscopy (values in parentheses indicate the uncertainties calculated from three independent experiments);
[g]FBSA immobilization efficiency (%) = FBSA loading$_{exp}$/FBSA loading$_{cal}$.

S5. Epitaxial growth of multi-core-shell FBSA/*sod*-Zn(mIM)$_2$ composites

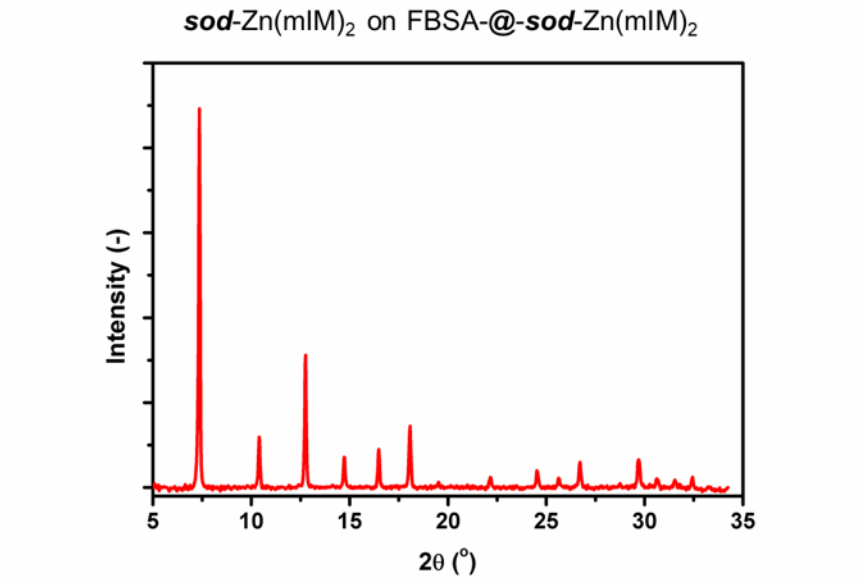

Figure S27. Experimental PXRD patterns for ***sod***-Zn(mIM)$_2$ on FBSA-***@-sod***-Zn(mIM)$_2$.

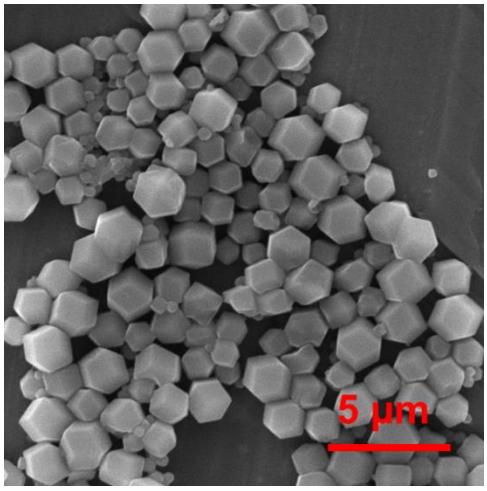

Figure S28. SEM images for ***sod***-Zn(mIM)$_2$ on FBSA-***@-sod***-Zn(mIM)$_2$. Particle size for the ***sod***-Zn(mIM)$_2$ on FBSA-***@-sod***-Zn(mIM)$_2$ sample was calculated to be 2.13 ± 0.21 µm) and the thickness of ***sod***-Zn(mIM)$_2$ shell was calculated to be 0.55 µm.

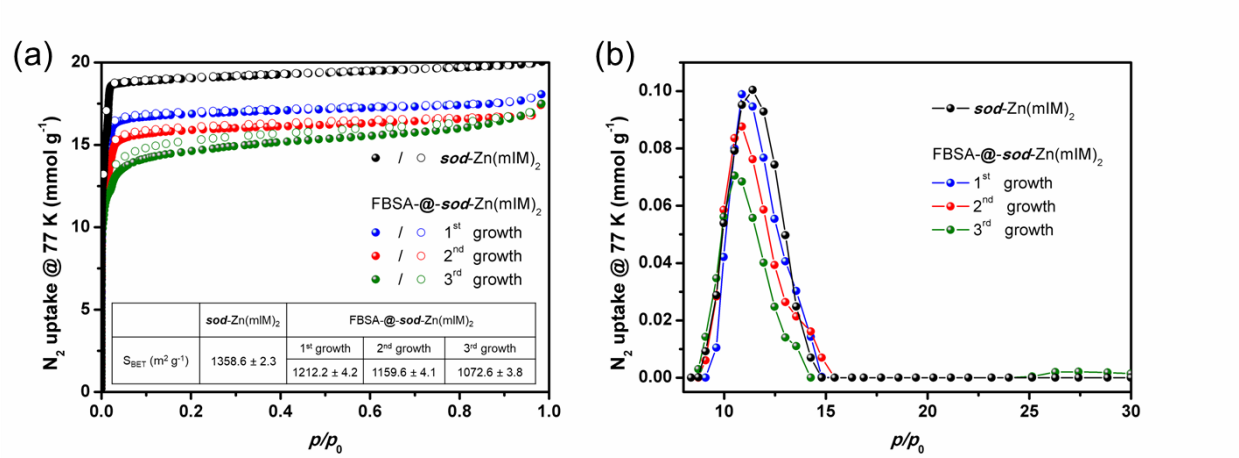

Figure S29. (a) 77K N_2 adsorption (filled symbol) desorption (open symbol) isotherms for ***sod***-Zn(mIM)$_2$ (black) and the epitaxial growth FBSA-@-***sod***-Zn(mIM)$_2$ samples (1st growth (blue), 2nd growth (red), and 3rd growth (green)). The calculated BET surface areas for samples are listed in the inset table. (b) NLDFT calculated pore size distribution curves for ***sod***-Zn(mIM)$_2$ (black) and the epitaxial growth FBSA-***@-sod***-Zn(mIM)$_2$ samples (1st growth (blue), 2nd growth (red), and 3rd growth (green)).

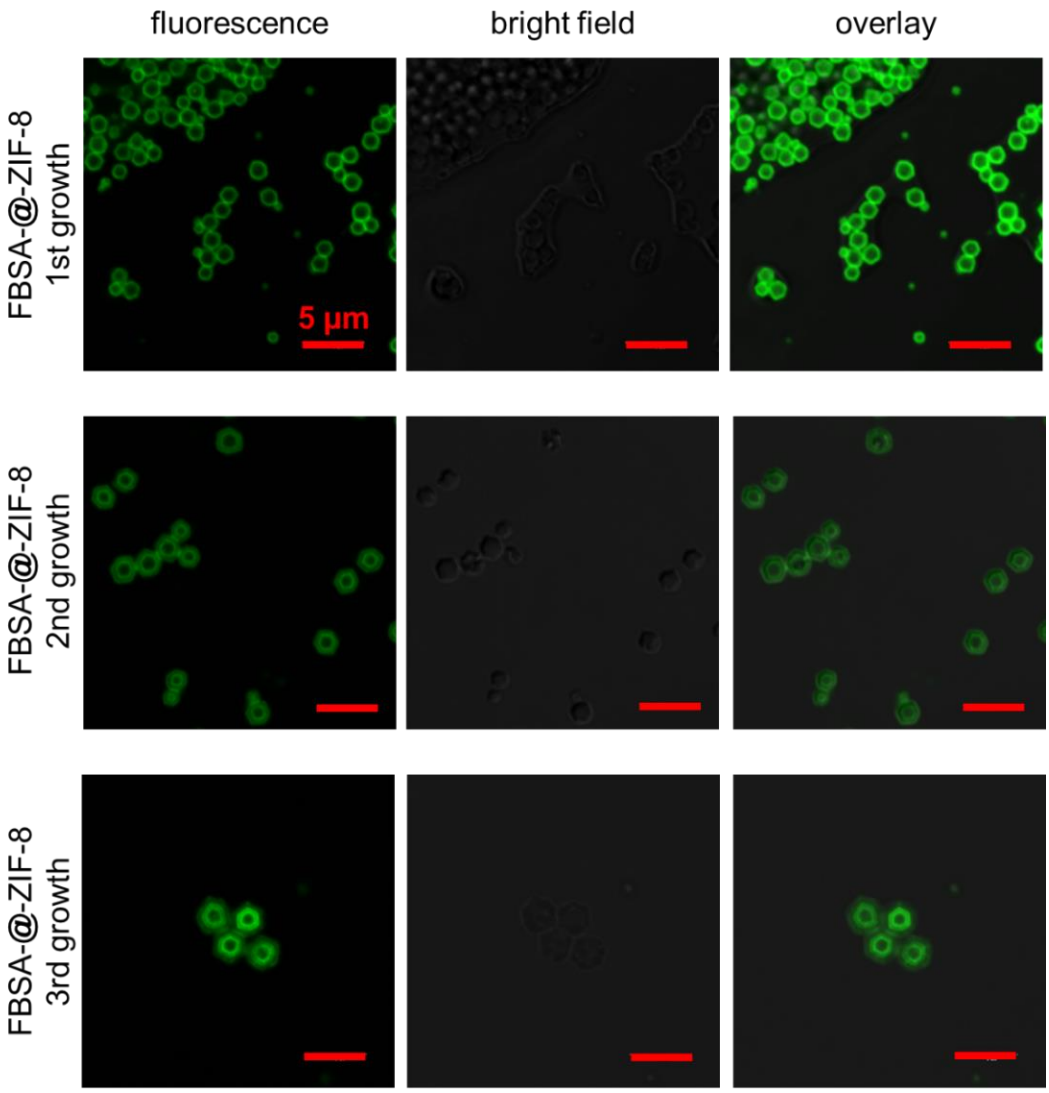

Figure S30. Confocal laser scanning micrographs showing the fluorescence, bright field, and overlay images of first, secondary, tertiary growth of FBSA-***@-sod***-Zn(mIM)$_2$, showing the multi-core-shell structures of the FBSA/ZIF-8 composites. Scale bar for all images is 5 µm.

S6. Enzymatic assay for HRP, FHRP, and FHRP released from FHRP-@-sod-Zn(mIM)$_2$ composite

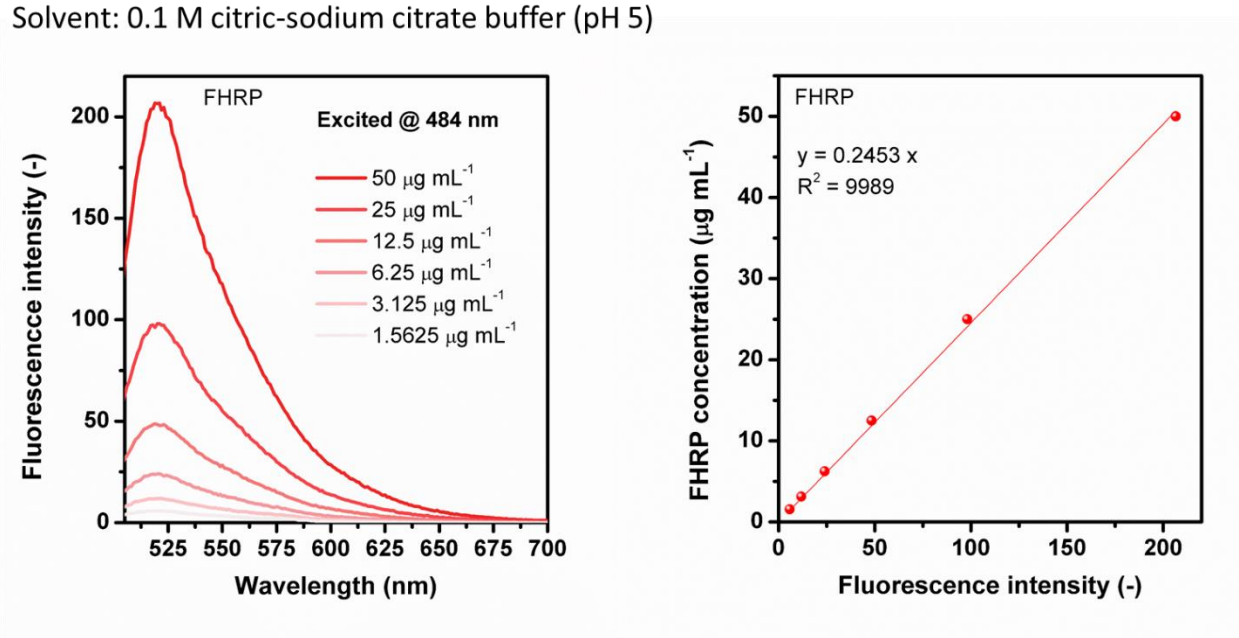

Figure S31. Calibration curve for FHRP in 0.1 M citric-sodium citrate buffer (pH 5).

The method for quantification of FHRP within the FHRP-***@-sod***-Zn(mIM)$_2$ composite is analogue to that of FBSA-***@-sod***-Zn(mIM)$_2$ (*vide supra*). The loading of FHRP within the FHRP-***@-sod***-Zn(mIM)$_2$ composite was determined to be 2.6 ± 0.2 wt%, and the encapsulation efficiency was calculated to be 75.6%.

In order to check whether the encapsulated FHRP is still active, we digested the FHRP-***@-sod***-Zn(mIM)$_2$ composite using 40 mM EDTA aqueous solution. The released FHRP was determined for its enzymatic activity using pyrogallol as substrate. In a typical experiment, 2.1 mL of water, 0.32 mL of phosphate buffer (0.1 M, pH 6.0), 0.16 mL of peroxide solution (0.50% (w/w)), 0.32 mL of pyrogallol solution (5%, w/v), and 0.1 mL of released FHRP solution (6.5 μg mL^{-1} FHRP) were added in sequence in a cuvette under magnetic stirring. Thereafter the absorbance at 420 nm was recorded for 5 minutes (5s interval, the reaction solution was under vigorous stirring during the whole period of time). The enzymatic activity of released FHRP was then compared to those of HRP and FHRP. The amount of HRP and FHRP used for assay analysis was the same as that of released FHRP (6.5 μg mL^{-1}).

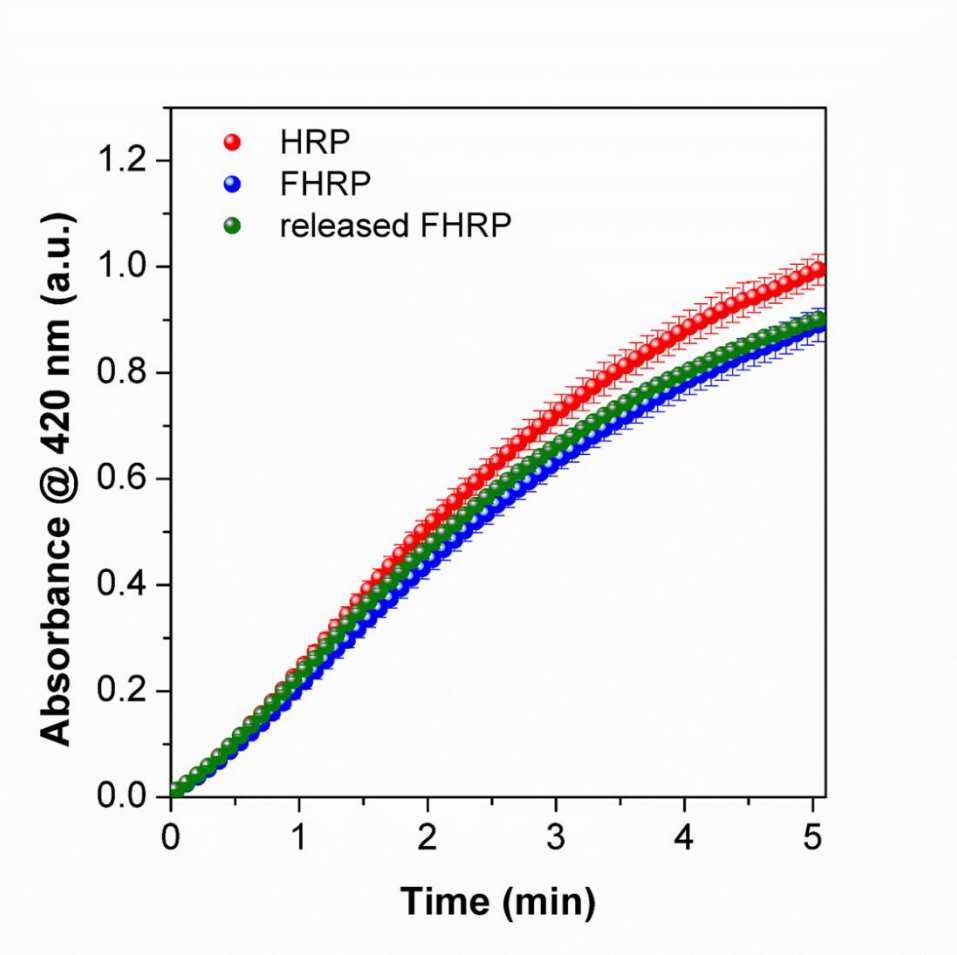

Figure S32. Time course curves for the enzymatic assay of HRP (red), FHRP (blue), and released FHRP from the FHRP-***@-sod***-Zn(mIM)$_2$ composite (green). Each experiment was repeated three times to ensure reproducibility.

Figure S32 shows that the FHRP preserved its catalytic activity after ZIF-8 encapsulation and post-synthetic washing treatment.